

Lignin alkaline oxidation using reversibly-soluble bases

Jacob S. Kruger,^a Reagan J. Dreiling,^a Daniel G. Wilcox,^a Arik J. Ringsby,^a Katherine L. Noon,^a Camille K. Amador,^a David G. Brandner,^a Kelsey J. Ramirez,^a Stefan J. Haugen,^a Bruno C. Klein,^b Ryan Davis,^b Rebecca J. Hanes,^b Renee M. Happs,^a Nicholas S. Cleveland,^a Earl D. Christensen,^b Joel Miscall,^a and Gregg T. Beckham^{a,*}

^a Renewable Resources and Enabling Sciences Center, National Renewable Energy Laboratory, 15013 Denver West Parkway, Golden, CO 80401 USA.

^b Catalytic Carbon Transformation and Scale-Up Center, National Renewable Energy Laboratory, 15013 Denver West Parkway, Golden, CO 80401 USA.

* E-mail: Gregg.Beckham@nrel.gov.

Abstract: Lignin valorization approaches, which are critical to biorefining, often involve depolymerization to aromatic monomers. Alkaline oxidation has long held promise as a lignin depolymerization strategy, but requires high concentrations of base, typically NaOH, much of which must be neutralized to recover lignin-derived aromatic monomers. This consumption of base and associated waste generation incurs high cost and negative environmental impacts. In this work, we demonstrate that Sr(OH)₂ and Ba(OH)₂ perform comparably to NaOH in terms of total aromatic monomer yields in the aqueous aerobic alkaline depolymerization of corn stover lignin, and that up to 90% of these reversibly-soluble bases can be recovered via precipitation and filtration. Process modeling suggests that the use of Sr(OH)₂ could reduce the cost of alkaline oxidation by 20-60% compared to NaOH, depending on lignin loading. In contrast, the energy required to regenerate the Sr largely offsets potential improvements in sustainability over Na-promoted alkaline oxidation, though the sustainability comparison is likely sensitive to the lignin composition and could be improved by further optimization of the regeneration step.

DOI: 10.1039/x0xx00000x

Table of Contents

Experimental Procedures.....	3
Results and Discussion.....	6

Figure S1. Schematic comparison of envisioned process compared to other lignin alkaline oxidation processes.

Figure S2. Stability of vanillin and p-hydroxybenzaldehyde under reaction conditions.

Figure S3. GPC profiles for native corn stover lignin before and after alkaline oxidation.

Figure S4. TGA profiles for SrCO₃ and BaCO₃.

Figure S5. 2D HSQC NMR spectra of native and depolymerized corn stover lignin.

Figure S6. Degradation of p-coumaric and ferulic acids under non-oxidizing conditions.

Figure S7. Neutralization of post-reaction hydroxide solutions using CO₂.

Figure S8. Monomer yields through process-relevant workup protocol.

Figure S9. GPC traces of the reactions solutions and residual insoluble solids from Sr(OH)₂-promoted oxidation of DMR-EH lignin.

Figure S10. Machine learning fit for optimization data.

Figure S11. Na- and Sr-based flowsheets for lignin oxidation.

Table S1. Numerical data corresponding to Figure 2.

Table S2. Numerical data corresponding to Figure 3.

Table S3. Numerical data corresponding to Figure S2.

Table S4. Numerical data corresponding to Figure 4.

Table S5. Numerical data corresponding to Figure S7.

Table S6. Compositional analysis of native corn stover, deacetylation black liquor, and DMR-EH residue.

Table S7. Numerical data corresponding to Figure 5.

Table S8. Numerical data corresponding to Figure S8.

Table S9. Numerical data corresponding to Figure 6.

Table S10. Numerical data corresponding to Figure 7.

Table S11. Numerical data corresponding to Figure 8.

Table S12. Main parameters used for process modeling.

Table S13. Financial assumptions used in the TEA, based on a mature nth plant design.

Table S14. Prices of the main inputs consumed in the processes.

Table S15. Numerical data corresponding to Figure 9.

Table S16. Sensitivity analysis towards lignin oxidation conditions.

Table S17. Numerical data corresponding to Figure 10.

Experimental Procedures

Materials

Corn stover enzymatic hydrolysis lignin was obtained from the NREL pilot plant. Subsequently, 125 kg corn stover was deacetylated in a 1,900 L paddle reactor using 80 mg NaOH/g stover and 8 wt% stover solids loading for 2 h at 90 °C. The deacetylated slurry was filtered to recover the deacetylation black liquor and the remaining residual cellulosic solids were partially washed prior to disk refining. These solids were mechanically refined in a 36" disk refiner at the Andritz pilot plant (Springfield, OH), and enzymatically hydrolyzed using 20 mg of Novozymes CTec3 and 5 mg HTec3/g cellulose in the deacetylated pulp (cellulose content was estimated at 46 wt%). The solid residue after enzymatic hydrolysis was isolated from the hydrolysate by centrifugation, washed with water until the carbohydrate content of the washes was < 2 g/L, and lyophilized for storage until use. This residue is called DMR-EH lignin. The composition of the DMR-EH lignin was determined by a series of analyses,¹ and is shown in **Table S6**. The lignin liberated during deacetylation was preserved by lyophilizing the deacetylation black liquor and analyzed for composition by the same protocols as the DMR-EH lignin. The parent corn stover was milled to 20 mesh in a Wiley mill and analyzed similarly.

Cellulose (Alcell), glucose (99%), NaOH (98%), Sr(OH)₂·8H₂O (98%), SrO (99%), SrCO₃ (99%) and Ba(OH)₂·8H₂O (98%), Ru/C (5 wt% Ru), N,O-bis(trimethylsilyl)trifluoroacetamide (BSTFA), DMSO-d₆, pyridine-d₅, and ethyl acetate (99%) were purchased from Sigma-Aldrich. Methanol (98%) and THF (99%) were purchased from Fisher.

Methods

Lignin Oxidation

In a typical reaction, lignin or biomass, solid base, and deionized water were added to a 75 mL Parr reactor, along with a stir bar. The reactor was sealed, purged with He, and checked for leaks, vented to the desired initial pressure of He, then heated to the desired reaction temperature. When at temperature, zero air was added to generate the desired total pressure. For typical reactions at 175 °C, the pressure inside the reactor when starting with 0 barg He was roughly 8 barg before adding air, implying that 30 bar total pressure would correspond to 22 barg partial pressure of air. To compare across temperatures and pressures during the optimization runs, heating was started with 2 bar He (when heating to 175 °C) or 4 bar He (when heating to 160 °C) initial pressures such that the air partial pressure would remain constant for the same total pressure across temperatures. After the desired oxidation time, the reactor was quenched in room temperature water.

Optimization experiments were designed using a Box-Behnken approach. This approach was chosen to minimize experimental runs while avoiding extremes that were likely to result in low monomer yields. Monomer yields from these experiments were regressed to a contour plot constructed using a radial basis function with gaussian fit machine learning algorithm in the scikit-learn Python package, adapting the code developed by Cao et al.² Model parameters: gamma = 0.2, epsilon = 0.001, C = 1.

Reactor Workup

When cool, reactors were depressurized, opened and the contents emptied into a ChemRus 60 mL filter funnel, and vacuum filtered to recover residual biomass and metal hydroxide. The solid cake was dried in air and reserved for analysis, while the liquid filtrate and stir bar were then returned to the Parr reactor. The reactor was again sealed and checked for leaks, and then pressurized with 35 bar CO₂ and stirred for 10 min at room temperature to neutralize the residual solution. The reactor was then vented and opened, the contents were emptied into a separate ChemRus 60 mL filter funnel, and vacuum filtered to recover precipitated carbonate.

HPLC Analysis

Samples were analyzed for aliphatic acids by high performance liquid chromatography with refractive index detection (HPLC-RID) and aromatic compounds by ultra-high performance liquid chromatography - tandem mass spectrometry (UHPLC-MS/MS) utilizing multiple reaction monitoring (MRM) for quantitation as previously described by Saboe et. al.³ Briefly, the aliphatic acid method employed an Agilent 1200 HPLC system with an Aminex HPX-87H 300 mm x 7.8 mm ion exclusion column maintained at 55 °C, using a 20 µL injection volume. The mobile phase was 0.02 N H₂SO₄, flow rate of 0.5 mL/min, and run time of 30 min. Calibration curves were constructed using commercially available standards at concentrations from 0.125 g/L to 5 g/L, and a calibration verification standard (CVS) was injected after every 15 injections to verify instrument stability. The UHPLC-MS/MS method was the same as previously reported,⁴ with the exception of 0.1% formic acid as the modifier in mobile phase A instead of 4 mM ammonium formate. Calibration curves with a minimum of eight levels were utilized for quantitation with r² coefficient values ≥ 0.995 and a CVS was analyzed every 10 samples to monitor instrument performance. Qualification and quantification MRM transitions and the respective collision energy and fragmentor voltage settings were also previously reported.⁵

Reductive Catalytic Fractionation and GC Analysis

To estimate maximum achievable monomer yields from the DMR-EH lignin, 0.3 g Ru/C (5 wt% Ru) was slurried with 0.5 mL deionized water in a 75 mL Parr batch reactor. To this slurry, 1 g DMR-EH residue and 30 mL methanol were added. The reactor was sealed, leak-checked, and pressurized with 30 bar H₂. Stirring was set to 800 rpm and the reactor was heated to 225 °C, held at that temperature

for 3 h, and then quenched in cool water. When the reactors were cool, the contents were filtered with a 0.2 μm syringe filter and mixed with an external standard of 1,3,5-tri-*tert*-butylbenzene in methanol and analyzed directly by GC-FID as described previously.⁶

Gel Permeation Chromatography (GPC)

To recover solubilized lignin as an oil, aqueous samples were acidified to pH 1 and extracted with ethyl acetate. The ethyl acetate was removed by rotary evaporation, and the resulting oil was acetylated using pyridine and acetic anhydride. The acetylated samples were then dried under nitrogen with periodic additions of methanol. Residual solids were then extracted directly with THF. The THF-soluble portions were then analyzed by size-exclusion chromatography, using polystyrene standards. The samples were injected onto three PLgel 7.5 x 300 mm columns in series: 10 μm x 50 \AA , 10 μm x 10³ \AA , 10 μm x 10⁴ \AA and monitored at 210 \pm nm, 260 \pm 40 nm and 270 \pm nm using a diode array detector.

Nuclear Magnetic Resonance (NMR) Spectroscopy

Samples were analyzed by the method of Mansfield *et al.*⁷ Briefly, 50 mg of each sample was directly dissolved in DMSO-d₆/pyridine-d₅ after ball milling to produce a gel. For the black liquor sample in D₂O, 55 mg of ball milled black liquor residuals were dissolved in D₂O. Less precipitates and better spectral quality were seen in this sample compared to the DMSO dissolved sample, presumably because any salts would solubilize easier in D₂O than DMSO. Heteronuclear single quantum coherence (HSQC) NMR spectra were acquired at 25 °C on a Bruker Avance III 300 MHz spectrometer at 7.05 T using a room temperature broadband probe. Spectra were acquired with 1,024 points and a SW of 12 ppm in the F2 (¹H) dimension and 256 points and SW of 220 ppm in the F1 (¹³C) dimension. The spectral processing parameters from Mansfield *et al.*⁷ were used. All spectral processing was done in Bruker Topspin 3.6.1.

Inductively Coupled Plasma Optical Emission Spectroscopy (ICP-OES) Analysis

After alkaline oxidation and precipitation of SrCO₃, liquid samples were analyzed for Sr content by ICP-OES. Liquid samples were stored at 4°C prior to analysis, during which time a precipitate formed. The precipitate was redissolved by mild heating (50°C), sonication, and vigorous shaking. Samples were then prepared for ICP via microwave assisted digestion using a CEM MARS 5 digester. Nominally 0.5 g of sample was digested with 10 mL of concentrated HNO₃ with 5 ppm Y added as an internal standard. The digester was operated at 1600 W and a temperature of 200°C held for 15 minutes (ramp to temperature in 15 minutes). Digested samples were then diluted with 18 M Ω DI water to a concentration within the instrument calibration range maintaining a consistent concentration of acid and internal standard. Prepared solutions were analyzed for Sr with an Agilent 5110 ICP-OES. Instrument conditions were as follows: axial viewing mode, RF power 1.40 kW, nebulizer flow 0.6 LPM, Ar plasma flow 13.0 LPM, auxiliary flow 1 LPM, viewing height 10 nm, read time 20 seconds, stabilization time 15 seconds, rinse time 90 seconds. Calibration was performed using a commercial standard (AccuStandard MES-04-1, 1,000 ppm) in a range of 0.05 to 20 ppm monitoring wavelengths 216.596 and 407.771 for Sr. Measurements were taken in 3 replicates and the average value of both bands was used to determine concentration.

Thermogravimetric Analysis (TGA)

Thermogravimetric Analysis (TGA) experiments were performed using a Discovery Series TGA 5500 (TA Instruments). Samples of 30-45 mg were loaded onto platinum pans for analysis. During analysis, the sample was purged with nitrogen gas at a flow rate of 25 mL/min. The sample was heated at a rate of 5 °C / min to a final temperature of 1000 °C. The sample was then held at 1000 °C for 30 minutes.

Recoverability

Recovery yields of the Sr(OH)₂ were determined gravimetrically on an anhydrous basis by drying the recovered Sr(OH)₂ and SrCO₃ in a vacuum oven at 40 °C for at least 2 h. It was determined that the octahydrate of Sr(OH)₂ partially converted to the monohydrate and anhydrous form during vacuum filtering operations, and thus full conversion to the anhydrous form provided the most reliable measure of hydroxide recovery.

Techno-Economic Analysis

Process simulations were built and run in Aspen Plus to generate mass and energy balances for processes. These are further used in determining the associated operational expenses (OPEX), as well as in estimating capital expenditures (CAPEX) with equipment purchase. The plants were sized to process the lignin obtained deacetylation and mechanical refining (DMR) pretreatment of corn stover in a biorefinery processing 2,000 dry tons of biomass per day,⁸ equivalent to 13 t/h of lignin. Process economics were estimated using the conditions presented in **Table S12** and the boundaries indicated in **Figure S11**. Results are given in terms of processing costs to achieve a mix of lignin monomers (\$/kg of lignin monomers), while considering the annualized CAPEX of the section (oxidation reactor, filters, neutralization reactor, calcination reactor, pumps, and ancillary equipment) as well as the OPEX (costs with steam for direct heating, base [either NaOH or SrCO₃], CO₂ for neutralization, natural gas, and electricity). No costs with feedstock (lignin) were considered.

Table S13 indicates the main assumptions used in the economic assessment. To reduce any uncertainties around Sr(OH)₂ prices (current prices found in the range of US\$ 1,300-3,000/t), sourcing Sr for the process passes through producing the hydroxide on-site using SrCO₃ as the starting point. Besides the fact that data for the carbonate is readily available (2016 import prices of US\$ 810/t), using a calcination reactor and starting from a material with much lower costs it would most likely improve process economics. Prices for the main inputs are shown in **Table S14**.

Sensitivity analysis. An additional assessment (not discussed in the main manuscript) investigated the effect of using milder reaction conditions and a shorter residence time on lignin processing costs. The smaller (and thus less expensive) reactor used in such scenarios does not offset the lower lignin monomer yield in the oxidation reaction (3.6% in comparison to 5.6% for the baseline case), leading to a 34% increase in processing costs. The findings are summarized in **Table S16**.

Life Cycle Assessment

Goal and scope definition. The goal of the life cycle assessment (LCA) is to determine the relative impact of base type and CO₂ recycling on global warming potential (GWP), cumulative energy demand (CED), and eco-toxicity of solubilized lignin. The goal is not to determine absolute environmental impacts, thus process inputs that are identical in quantity across the five process cases have been deliberately excluded from the scope. The only process input excluded for this reason is the biomass feedstock. For the remainder of the process, the LCA scope is cradle-to-gate, meaning that production and transportation of process inputs is included in the scope, and any downstream processing of solubilized lignin into other products is excluded from the scope. The functional unit of the LCA is the production of 1 kg solubilized lignin. Because the solubilized lignin is the only process output analyzed, no impact allocation is required.

Inventory analysis and assumptions. The inventory analysis was performed with the SimaPro software version 9.0.0.48. Background processes not explicitly mentioned here are sourced from the DATASMART background life cycle inventory database.⁹ In general, when assumptions are needed to complete the inventory or choose upstream processes, the assumptions are chosen to provide a conservative (high) estimate of environmental impacts.

Steam is assumed to be produced from lignin combustion, sourced from the same feedstock as the solubilized lignin. The emission factors used for lignin combustion were the GREET 2020 emission factors for switchgrass combusted in a large industrial boiler.¹⁰ The quantity of switchgrass required for steam combustion was calculated using the fuel energy content required for steam production in the "steam, for chemical processes, at plant" DATASMART activity and the lower heating value (LHV) of switchgrass sourced from GREET 2020. The amount of water required for steam generation was also calculated from the aforementioned DATASMART activity. Because the rate of steam recycle was unknown at the time of analysis, the water used for steam generation was treated as an input. The amount of switchgrass required for steam combustion did vary across the five cases, and so production, harvest, and transportation of switchgrass for steam combustion was included in the LCA system boundary.¹¹

Strontium carbonate is purchased for Sr(OH)₂ production within the process. Liquid carbon dioxide for carbonation is also purchased externally. Electricity for process use is purchased from an average U.S. electricity grid mix process. No electricity is exported from the process.

Impact assessment. The impacts quantified in this study are 100-year global warming potential, cumulative energy demand, and eco-toxicity. Because the amount of biomass combustion for steam varies across the five process cases, biogenic emissions from this combustion were also included in the GWP calculation, as were process-level CO₂ emissions from carbonation and from process leakages. Eco-toxicity is quantified in units of disability-adjusted life years (DALY) according to the USEtox 2 (recommended + interim) V1.00 methodology.¹²

Results and Discussion

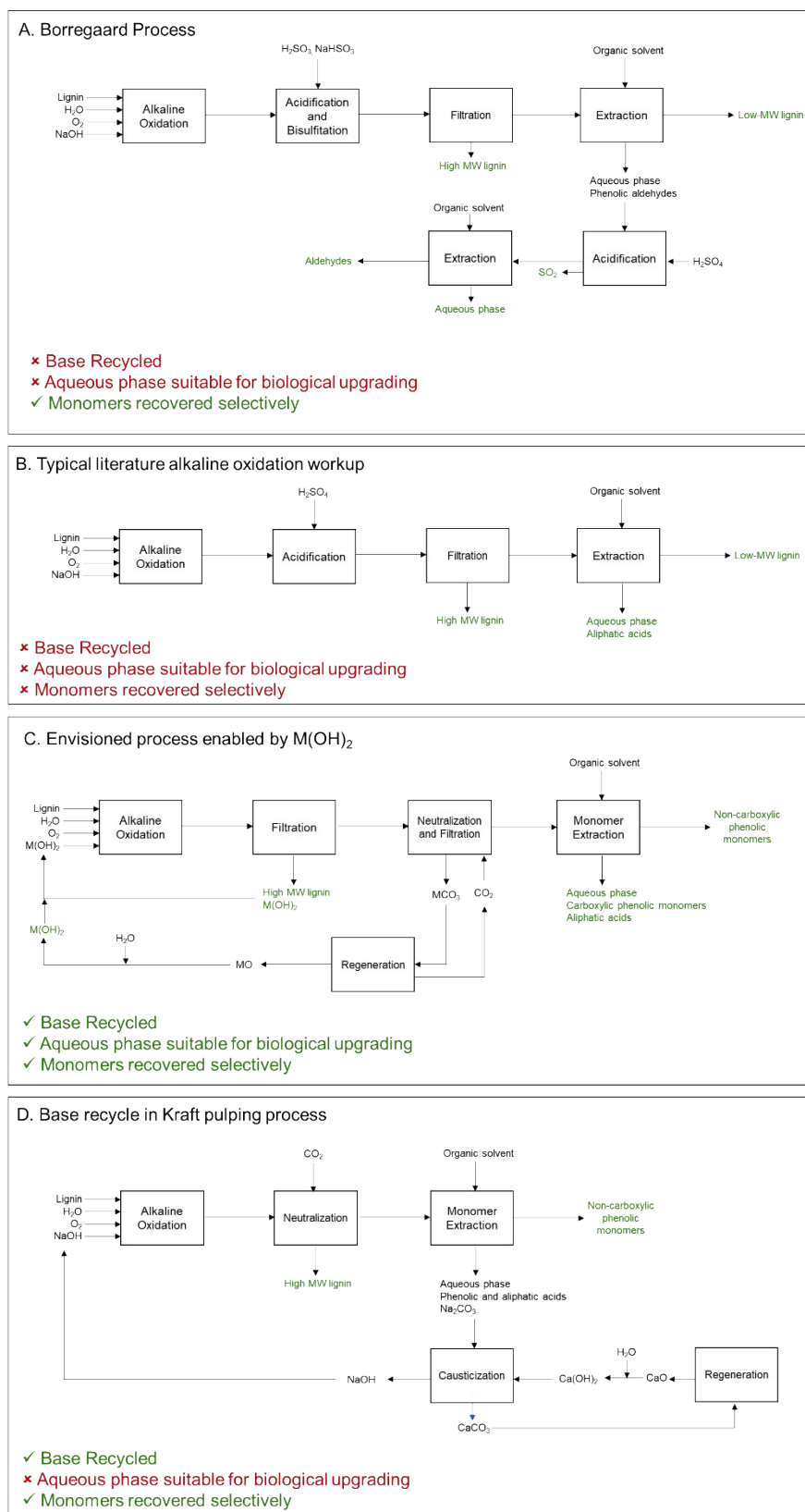


Figure S1. Potential scenarios for valorization of lignin by aqueous alkaline oxidation. A. Simplified Borregaard process employing bisulfitation for selective aldehyde recovery.¹³ B. Typical workup procedure in lignin alkaline oxidation literature. C. Envisioned process employing reversibly-soluble bases, where M = Sr or Ba. D. Process employing NaOH recycle using a lime cycle as in Kraft pulping.

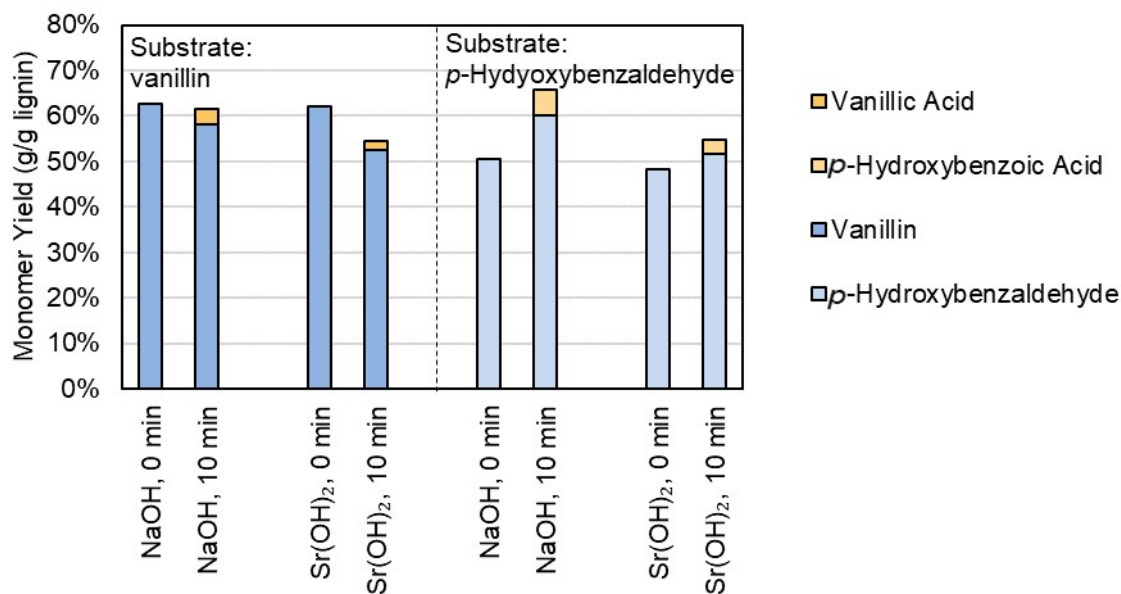


Figure S2. Fate of p-OH benzaldehyde and vanillin under alkaline oxidation conditions in the presence of NaOH or Sr(OH)₂. 0 min time points were quenched before adding O₂; 10 min time points had 22 bar air added upon reaching 175 °C. Numerical data for this figure given in Table S3.

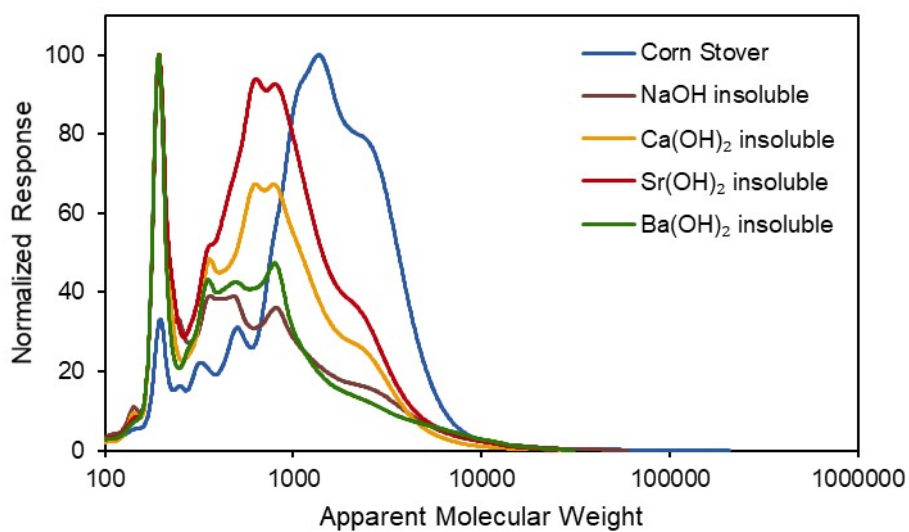


Figure S3. Gel permeation chromatograms for parent corn stover and insoluble residue after alkaline oxidation from NaOH and alkaline earth hydroxides.

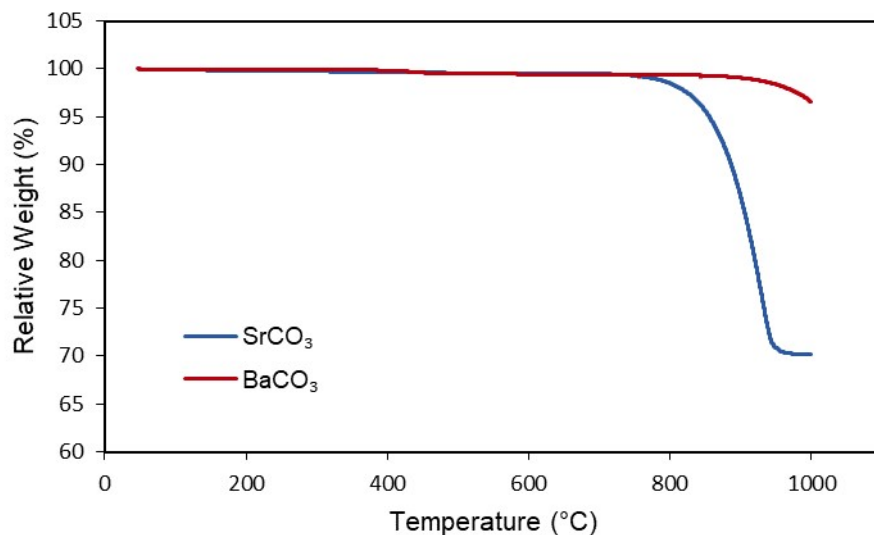


Figure S4. TGA profiles for SrCO_3 and BaCO_3 .

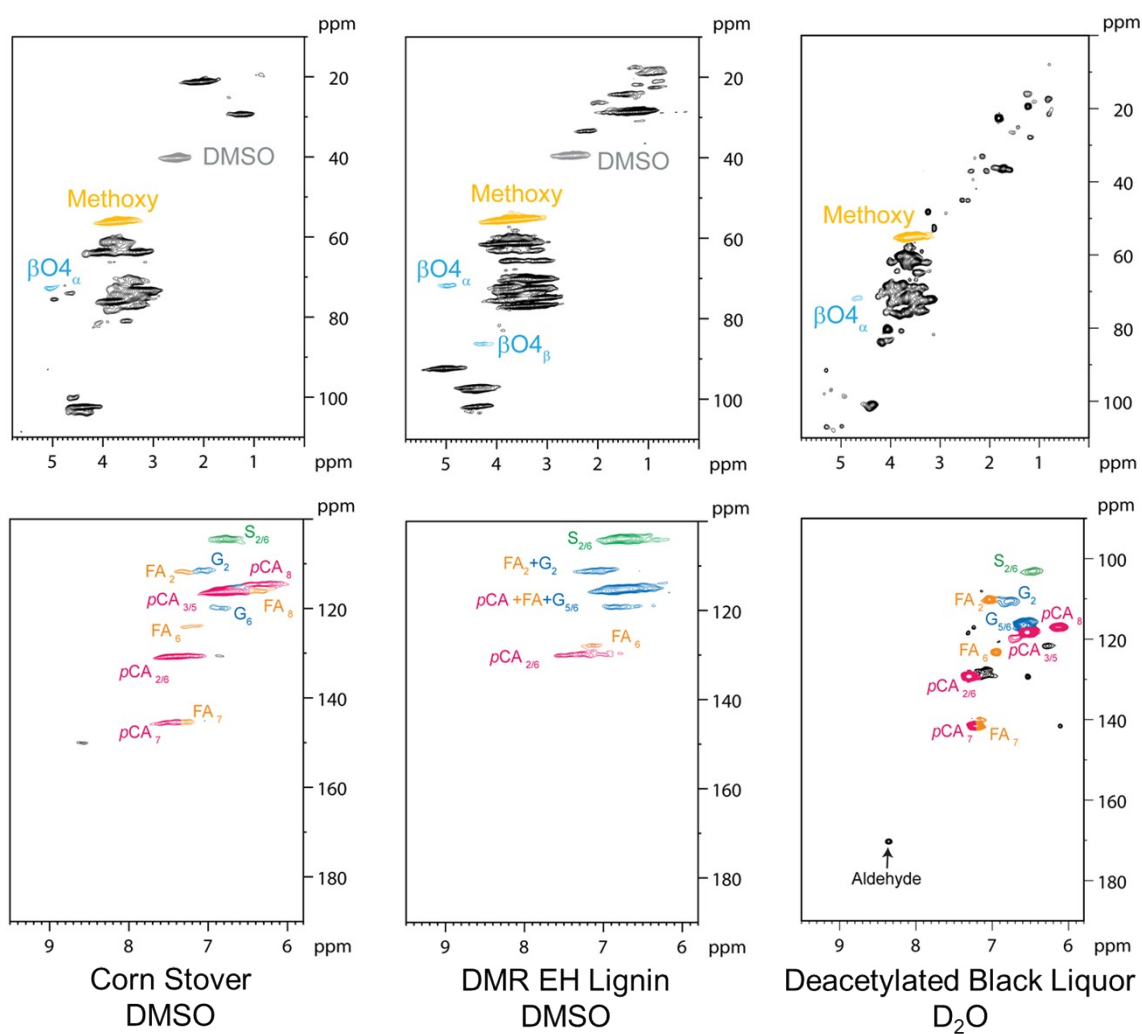


Figure S5. 2D HSQC NMR spectra of parent corn stover, solid DMR-EH residue, and deacetylated black liquor. Corn stover and DMR-EH lignin were dissolved in $\text{DMSO-}d_6/\text{pyridine-}d_5$, while deacetylated black liquor was dissolved in D_2O to improve spectral quality.

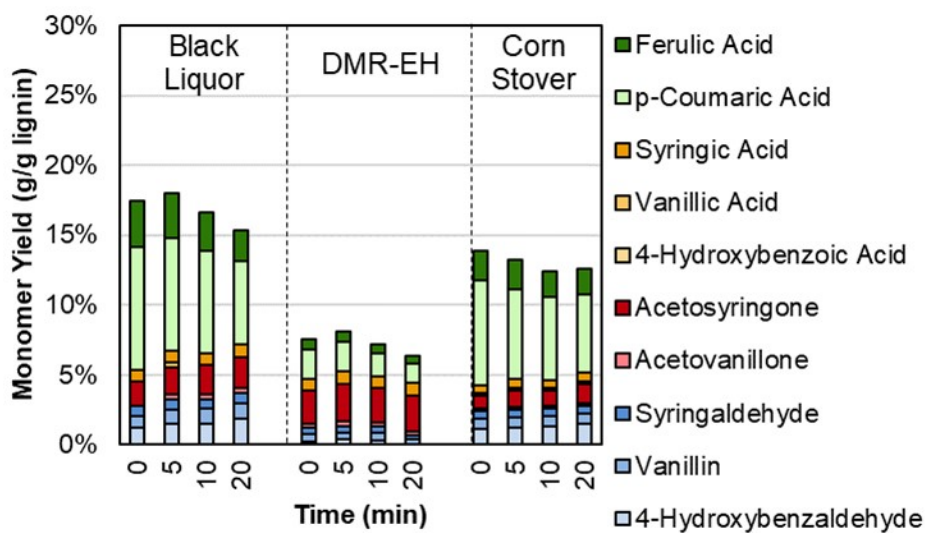


Figure S6. Lignin decomposition under alkaline oxidation conditions but without O_2 present. Reaction conditions: 1 g corn stover or 0.3 g isolated lignin, 7.9727 g $Sr(OH)_2 \cdot 8H_2O$, 30 mL H_2O , 175 °C, 10 min, He headspace. Numerical data for this figure given in Table S5.

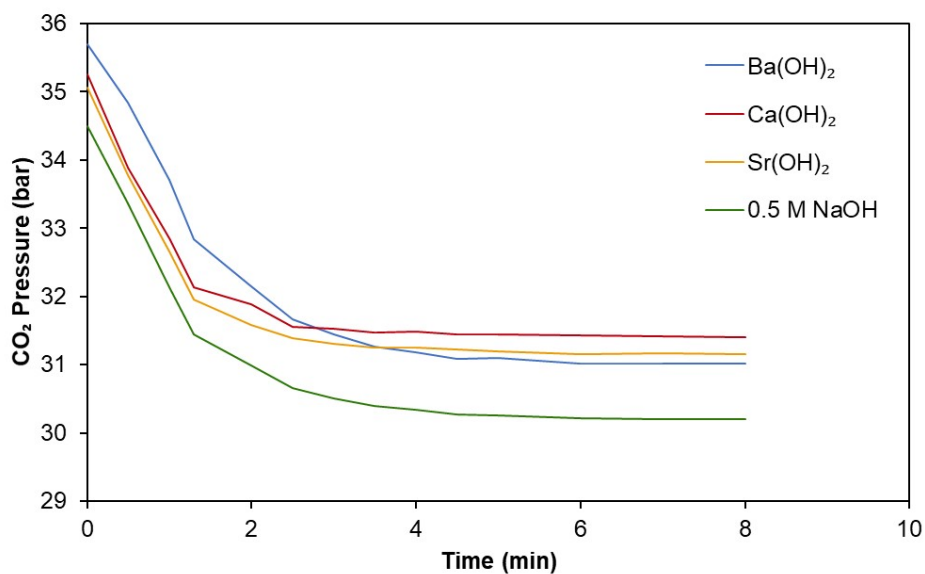


Figure S7. Neutralization kinetics of alkaline solutions using CO_2 .

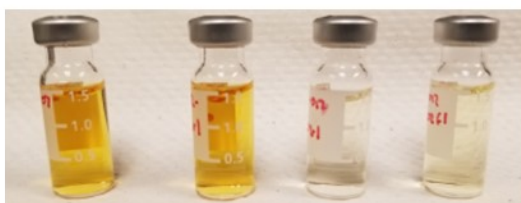
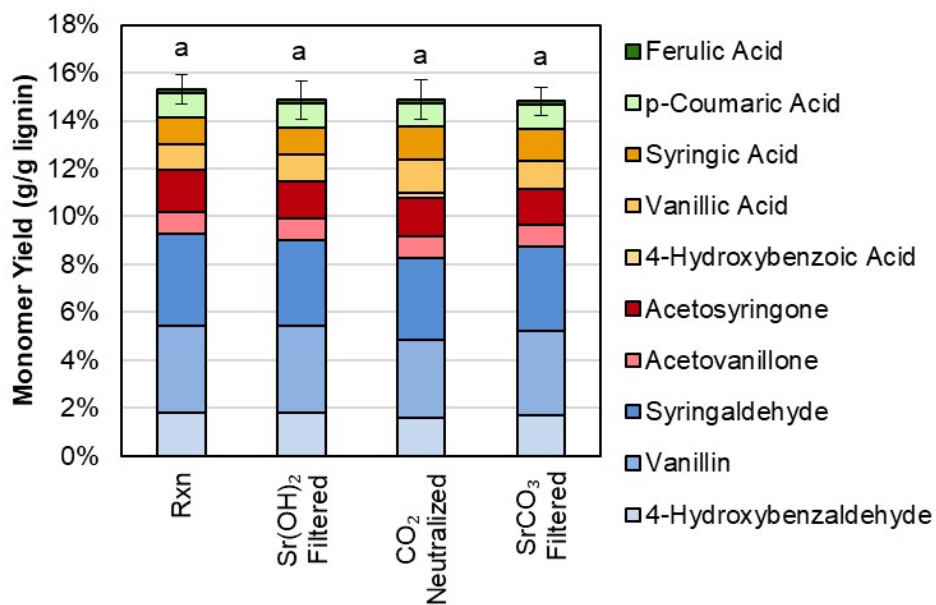


Figure S8. Monomer yields and solution appearance through neutralization and filtration workup protocols. Numerical data for this figure given in Table S8. The selective precipitation of oligomers during neutralization is supported by the gel permeation chromatograms shown in Figure S9.

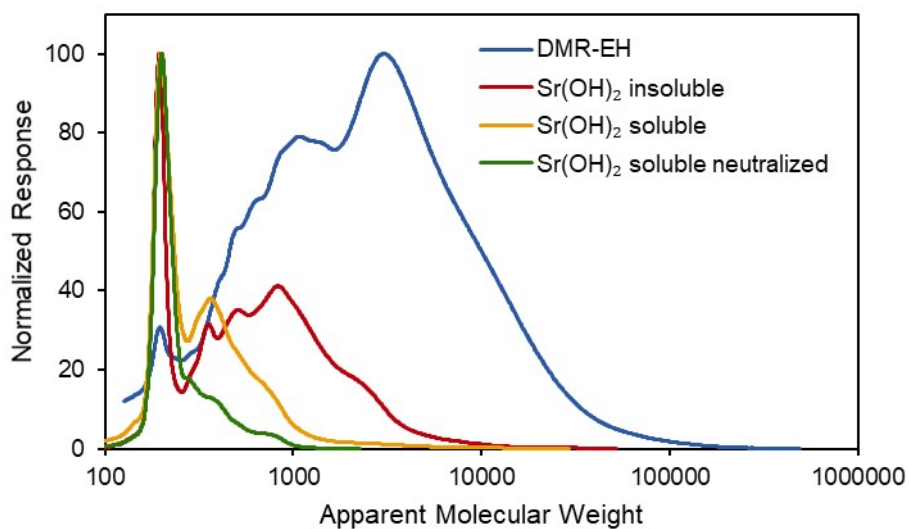


Figure S9. Gel permeation chromatograms of the reactions solutions and residual insoluble solids from Sr(OH)₂-promoted oxidation of DMR-EH lignin. After neutralization, oligomers are relatively less abundant, indicating that they precipitate along with SrCO₃.

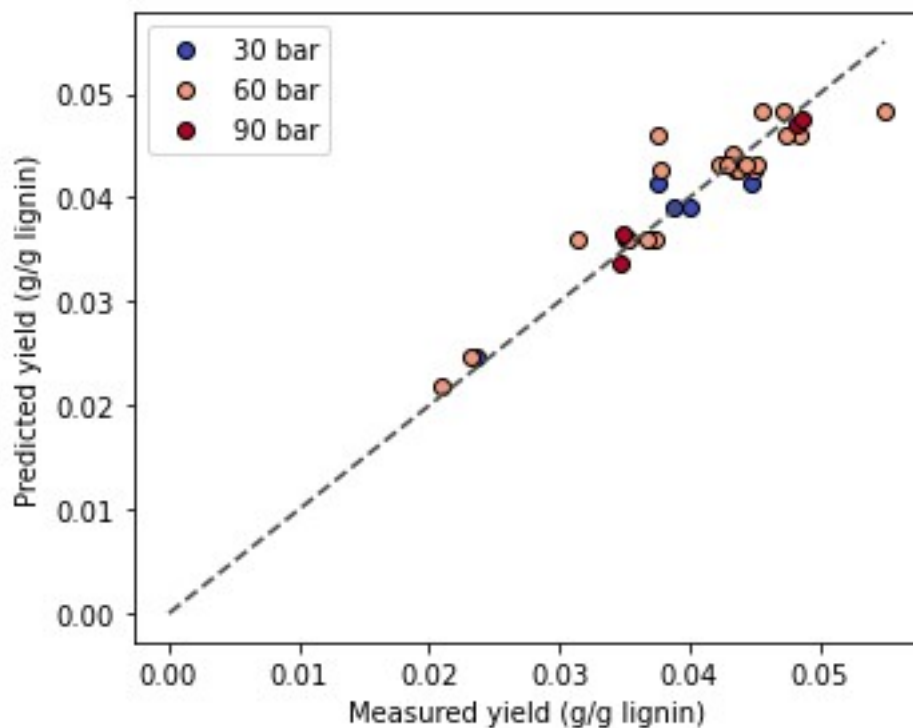


Figure S10. Machine learning fit for data in Figure 6.

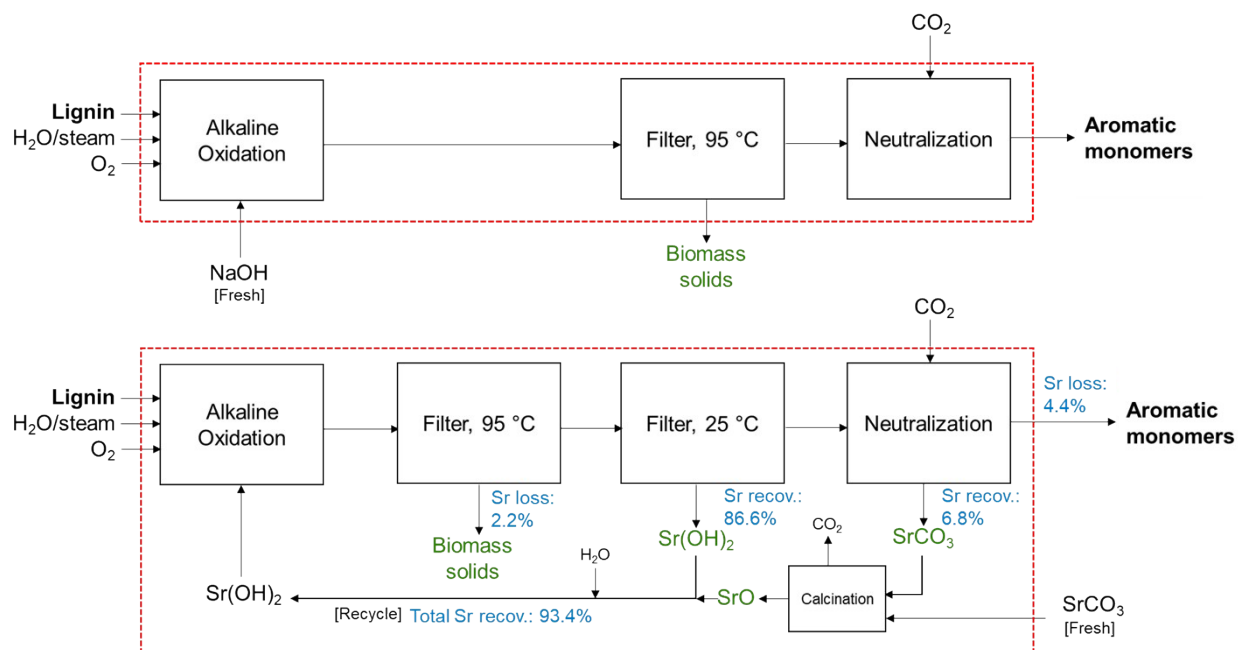


Figure S11. Na- and Sr-based flowsheets for lignin oxidation. TEA boundaries are shown in red.

Table S1. Numerical data corresponding to Figure 2.

Monomer	NaOH	Ca(OH) ₂	Sr(OH) ₂	Ba(OH) ₂
4-Hydroxybenzaldehyde	0.7%	1.6%	2.1%	1.3%
Vanillin	1.8%	1.5%	2.9%	2.2%
Syringaldehyde	2.8%	0.6%	2.5%	2.4%
Acetovanillone	0.5%	0.4%	0.6%	0.5%
Acetosyringone	2.7%	0.1%	1.5%	1.9%
4-Hydroxybenzoic Acid	0.1%	0.5%	0.2%	0.1%
Vanillic Acid	0.3%	0.3%	0.5%	0.4%
Syringic Acid	1.0%	0.0%	1.2%	1.1%
p-Coumaric Acid	10.0%	0.1%	5.7%	6.9%
Ferulic Acid	3.3%	0.0%	1.8%	2.3%
Total	23.1%	5.1%	19.0%	19.2%
Error Bars	4.4%	2.1%	1.6%	2.6%

Table S2. Numerical data corresponding to Figure 3.

Feed	p-Coumaric Acid				Ferulic Acid			
	NaOH 0 min	NaOH, 10 min	Sr(OH) ₂ 0 min	Sr(OH) ₂ 10 min	NaOH 0 min	NaOH 10 min	Sr(OH) ₂ 0 min	Sr(OH) ₂ 10 min
4-Hydroxybenzaldehyde	0.3%	10.3%	0.4%	1.9%	0.0%	0.0%	0.0%	0.0%
Vanillin	0.0%	0.0%	0.0%	0.0%	0.6%	8.1%	0.0%	4.6%
Syringaldehyde	0.0%	0.0%	0.0%	0.0%	0.0%	0.0%	0.0%	0.0%
Acetovanillone	0.0%	0.0%	0.0%	0.0%	0.7%	1.8%	0.2%	0.6%
Acetosyringone	0.0%	0.0%	0.0%	0.0%	0.6%	0.4%	0.0%	0.0%
4-Hydroxybenzoic Acid	0.0%	0.6%	0.0%	0.1%	0.0%	0.0%	0.0%	0.0%
Vanillic Acid	0.0%	0.0%	0.0%	0.0%	0.0%	0.5%	0.0%	1.0%
Syringic Acid	0.0%	0.0%	0.0%	0.0%	0.0%	0.0%	0.0%	0.0%
p-Coumaric Acid	63.9%	46.0%	13.5%	14.7%	0.0%	0.1%	0.0%	0.0%
Ferulic Acid	0.0%	0.0%	0.0%	0.0%	61.4%	39.2%	14.3%	8.0%
Total	64.2%	56.9%	13.9%	16.6%	63.3%	50.0%	14.5%	14.2%
Error Bars	2.5%				0.8%			

Table S3. Numerical data corresponding to Figure S2.

Feed	Vanillin				p-Hydroxybenzaldehyde			
	NaOH 0 min	NaOH, 10 min	Sr(OH) ₂ 0 min	Sr(OH) ₂ 10 min	NaOH 0 min	NaOH 10 min	Sr(OH) ₂ 0 min	Sr(OH) ₂ 10 min
4-Hydroxybenzaldehyde	0.0%	0.0%	0.0%	0.0%	50.5%	60.2%	48.2%	51.7%
Vanillin	62.8%	58.1%	62.2%	52.6%	0.0%	0.0%	0.0%	0.0%
Syringaldehyde	0.0%	0.0%	0.0%	0.0%	0.0%	0.0%	0.0%	0.0%
Acetovanillone	0.0%	0.0%	0.0%	0.0%	0.0%	0.0%	0.0%	0.0%
Acetosyringone	0.0%	0.0%	0.0%	0.0%	0.0%	0.0%	0.0%	0.0%
4-Hydroxybenzoic Acid	0.0%	0.0%	0.0%	0.0%	0.0%	5.4%	0.0%	3.1%
Vanillic Acid	0.0%	3.4%	0.0%	2.0%	0.0%	0.0%	0.0%	0.0%
Syringic Acid	0.0%	0.0%	0.0%	0.0%	0.0%	0.0%	0.0%	0.0%
p-Coumaric Acid	0.0%	0.0%	0.0%	0.0%	0.0%	0.0%	0.0%	0.0%
Ferulic Acid	0.0%	0.0%	0.0%	0.0%	0.0%	0.0%	0.0%	0.0%
Total	62.8%	61.5%	62.2%	54.6%	50.5%	65.7%	48.2%	54.8%

Table S4. Numerical data corresponding to Figure 4.

Monomer	Corn Stover 0 min	Black Liquor 0 min	DMR-EH 0 min	Corn Stover 10 min	Black Liquor 10 min	DMR-EH 10 min
4-Hydroxybenzaldehyde	0.8%	1.4%	0.0%	2.1%	5.8%	1.7%
Vanillin	0.6%	0.9%	0.4%	2.9%	5.9%	3.1%
Syringaldehyde	0.5%	1.0%	0.6%	2.5%	4.4%	3.5%
Acetovanillone	0.1%	0.3%	0.2%	0.6%	1.3%	0.9%
Acetosyringone	0.6%	1.6%	1.4%	1.5%	2.2%	2.1%
4-Hydroxybenzoic Acid	0.0%	0.1%	0.0%	0.2%	0.8%	0.1%
Vanillic Acid	0.1%	0.3%	0.2%	0.5%	1.6%	1.0%
Syringic Acid	0.4%	0.9%	0.8%	1.2%	0.6%	1.6%
p-Coumaric Acid	7.1%	8.8%	2.1%	5.7%	2.5%	1.0%
Ferulic Acid	2.2%	3.5%	0.8%	1.8%	0.1%	0.3%
Total	12.6%	18.9%	6.5%	19.0%	25.2%	15.1%
Error Bars	1.2%	0.7%	0.1%	1.6%	1.1%	0.6%

Table S5. Numerical data corresponding to Figure S6.

Substrate	Black Liquor				DMR-EH			
	0 min	5 min	10 min	20 min	0 min	5 min	10 min	20 min
4-Hydroxybenzaldehyde	1.2%	1.5%	1.5%	1.9%	0.2%	0.4%	0.3%	0.1%
Vanillin	0.9%	1.0%	1.0%	1.1%	0.5%	0.5%	0.5%	0.3%
Syringaldehyde	0.7%	0.7%	0.7%	0.7%	0.5%	0.5%	0.5%	0.3%
Acetovanillone	0.0%	0.3%	0.3%	0.3%	0.2%	0.3%	0.3%	0.3%
Acetosyringone	1.8%	2.0%	2.1%	2.2%	2.3%	2.7%	2.5%	2.5%
4-Hydroxybenzoic Acid	0.0%	0.0%	0.0%	0.0%	0.0%	0.0%	0.0%	0.0%
Vanillic Acid	0.0%	0.3%	0.0%	0.0%	0.0%	0.0%	0.0%	0.0%
Syringic Acid	0.8%	0.9%	0.9%	0.9%	0.8%	1.0%	0.8%	0.9%
p-Coumaric Acid	8.8%	8.1%	7.3%	5.9%	2.1%	2.1%	1.7%	1.5%
Ferulic Acid	3.3%	3.2%	2.8%	2.3%	0.7%	0.7%	0.6%	0.6%
Total	17.4%	18.0%	16.7%	15.4%	7.5%	8.1%	7.2%	6.4%

Substrate	Corn Stover			
	0 min	10 min	5 min	20 min
4-Hydroxybenzaldehyde	1.1%	1.2%	1.3%	1.5%
Vanillin	0.7%	0.7%	0.7%	0.8%
Syringaldehyde	0.6%	0.6%	0.5%	0.5%
Acetovanillone	0.2%	0.2%	0.2%	0.2%
Acetosyringone	0.9%	1.2%	1.1%	1.3%
4-Hydroxybenzoic Acid	0.1%	0.1%	0.1%	0.1%
Vanillic Acid	0.1%	0.2%	0.1%	0.2%
Syringic Acid	0.5%	0.6%	0.5%	0.6%
p-Coumaric Acid	7.5%	6.5%	6.0%	5.6%
Ferulic Acid	2.2%	2.0%	1.8%	1.8%
Total	13.9%	13.2%	12.4%	12.6%

Table S6. Compositional analysis of corn stover, deacetylation black liquor, and DMR-EH lignin feedstocks.

Fraction	Corn Stover	DMR-EH	Black Liquor
%Total Ash	6.97	10.9	29.41
%Total Protein	2.67	6.49	4.25
% Lignin	18.16	41.35	33.63
% Glucan	36.23	27.74	3.62
% Xylan	21.34	10.21	10.24
% Galactan	1.61	1.83	2.09
% Arabinan	3.25	1.67	4.29
% Acetyl	2.15	0.24	4.49
Total %	92.37	100.42	92.01

Table S7. Numerical data corresponding to Figure 5.

Substrate	Glucose, no O ₂				Cellulose, no O ₂			
	0 min	5 min	10 min	20 min	0 min	5 min	10 min	20 min
Formic Acid	5.2%	5.6%	5.8%	5.5%	1.4%	1.6%	1.8%	1.7%
Acetic Acid	4.6%	4.6%	4.9%	4.4%	1.5%	1.6%	1.9%	1.8%
Glycolic Acid	3.1%	2.8%	2.9%	3.0%	0.0%	0.0%	0.0%	1.3%
Oxalic Acid	0.0%	0.0%	0.0%	0.0%	0.0%	0.0%	0.0%	0.0%
Propionic Acid	0.0%	0.0%	0.0%	0.0%	0.0%	0.0%	0.0%	0.0%
Lactic Acid	43.0%	44.5%	42.7%	43.6%	2.3%	2.5%	2.8%	3.2%
Malonic Acid	1.8%	1.9%	1.7%	1.6%	0.0%	0.0%	0.0%	0.0%
Succinic Acid	0.0%	0.0%	0.0%	0.0%	0.0%	0.0%	0.0%	0.0%
Fumaric Acid	1.7%	2.0%	1.9%	1.6%	0.0%	0.0%	0.0%	0.0%
Malic Acid	0.0%	0.0%	0.0%	0.0%	0.0%	0.0%	0.0%	0.0%
Total	59.4%	61.4%	59.9%	59.7%	5.1%	5.7%	6.4%	8.0%

Substrate	Glucose, O ₂			Cellulose, O ₂			
	0 min	10 min	20 min	0 min	5 min	10 min	20 min
Formic Acid	4.7%	8.4%	8.7%	0.0%	5.4%	3.5%	10.0%
Acetic Acid	4.0%	7.1%	6.6%	1.5%	3.0%	2.5%	5.6%
Glycolic Acid	3.5%	4.9%	4.7%	0.0%	4.3%	2.5%	2.5%
Oxalic Acid	0.0%	0.0%	0.0%	0.0%	0.0%	0.0%	0.0%
Propionic Acid	0.0%	0.0%	0.0%	0.0%	0.0%	0.0%	0.0%
Lactic Acid	44.2%	50.1%	50.1%	2.2%	8.1%	5.1%	11.9%
Malonic Acid	1.8%	0.0%	0.0%	0.0%	0.0%	0.0%	0.0%
Succinic Acid	0.0%	0.0%	0.0%	0.0%	0.0%	0.0%	0.0%
Fumaric Acid	1.6%	2.3%	1.8%	0.0%	1.4%	1.5%	1.4%
Malic Acid	0.0%	0.0%	0.0%	0.0%	0.0%	0.0%	0.0%
Total	59.8%	72.8%	72.0%	3.8%	22.2%	15.3%	31.4%

Table S8. Numerical data corresponding to Figure S8.

Product	Reactor	Sr(OH) ₂ Filtered	CO ₂ Neutralized	SrCO ₃ Filtered
4-Hydroxybenzaldehyde	1.8%	1.8%	1.6%	1.7%
Vanillin	3.7%	3.6%	3.3%	3.5%
Syringaldehyde	3.8%	3.6%	3.4%	3.5%
Acetovanillone	0.9%	0.9%	0.9%	0.9%
Acetosyringone	1.8%	1.6%	1.6%	1.5%
4-Hydroxybenzoic Acid	0.0%	0.0%	0.2%	0.0%
Vanillic Acid	1.1%	1.1%	1.4%	1.2%
Syringic Acid	1.1%	1.1%	1.4%	1.3%
p-Coumaric Acid	1.0%	1.0%	1.0%	1.0%
Ferulic Acid	0.1%	0.1%	0.1%	0.1%
Total	15.3%	14.9%	14.9%	14.8%
Error Bars	0.6%	0.8%	0.8%	0.6%

Table S9. Numerical data corresponding to Figure 6.

Monomer	Sr(OH) ₂	None	SrCO ₃	SrO	Calcined SrCO ₃
4-Hydroxybenzaldehyde	1.7%	0.4%	0.2%	2.3%	2.5%
Vanillin	3.1%	0.5%	0.3%	4.1%	4.1%
Syringaldehyde	3.5%	0.4%	0.4%	3.9%	4.1%
Acetovanillone	0.9%	0.0%	0.0%	1.1%	1.1%
Acetosyringone	2.1%	0.0%	0.1%	1.7%	1.4%
4-Hydroxybenzoic Acid	0.1%	0.0%	0.3%	0.1%	0.1%
Vanillic Acid	1.0%	0.4%	0.5%	1.5%	1.5%
Syringic Acid	1.6%	0.4%	0.5%	1.6%	1.2%
p-Coumaric Acid	1.0%	0.0%	0.1%	0.9%	0.7%
Ferulic Acid	0.2%	0.0%	0.0%	0.2%	0.0%
Total	15.1%	2.2%	2.4%	17.4%	16.7%
Error Bars	1.1%	0.1%	0.4%	0.8%	1.1%

Table S10. Numerical data corresponding to Figure 7.

Monomer	Cycle 1	Cycle 2	Cycle 3
4-Hydroxybenzaldehyde	1.6%	2.0%	2.0%
Vanillin	3.2%	4.1%	4.1%
Syringaldehyde	3.3%	4.1%	4.2%
Acetovanillone	0.9%	1.2%	1.3%
Acetosyringone	2.0%	2.6%	2.8%
4-Hydroxybenzoic Acid	0.1%	0.3%	0.3%
Vanillic Acid	1.0%	1.3%	1.3%
Syringic Acid	1.3%	1.3%	1.5%
p-Coumaric Acid	0.9%	0.9%	0.9%
Ferulic Acid	0.3%	0.2%	0.3%
Total	14.6%	17.2%	19.0%
Positive Error Bars	0.6%	1.3%	0.0%
Negative Error Bars	0.3%	0.9%	0.0%

Table S11. Numerical data corresponding to Figure 8.

Time (min)	Temperature (°C)	Pressure (bar)	Total Monomer Yield (wt% lignin)
20	160	30	4.48%
20	190	30	2.37%
10	175	30	3.72%
30	175	30	3.99%
20	160	30	3.77%
10	175	30	3.52%
30	175	30	3.89%
10	160	60	4.34%
10	190	60	2.09%
30	160	60	5.50%
30	160	60	4.72%
30	160	60	4.57%
30	190	60	2.31%
20	175	60	4.84%
20	175	60	4.74%
20	175	60	3.76%
20	145	60	3.74%
20	145	60	3.53%
40	145	60	4.49%
40	145	60	4.34%
50	160	60	4.51%
50	160	60	4.22%
20	145	60	3.68%
20	145	60	3.14%
40	145	60	4.37%
40	145	60	3.78%
50	160	60	4.44%
50	160	60	4.30%
20	160	90	4.82%
20	190	90	3.48%
10	175	90	4.86%
30	175	90	3.50%

Table S12. Main parameters of the assessed processes.

Inputs	Na-based process	Sr-based system
Lignin loading (g/L)	10 or 100 (baseline)	10 or 100
Pressure (bar)	30	30
Temperature (°C)	175	175
Residence time (min)	30	30
Base concentration (M)	2	2
Base recovery	0%	93.4%
Stoichiometric CO ₂ excess in base neutralization	10%	10%

Table S13. Financial assumptions used in the TEA, based on a mature *n*th plant design.

Financial assumptions	Value
Capital charge factor	0.129 ^a
Cost year dollar	2016\$
Operational period	7884 h/year (90% on-stream factor)

^a Based on Davis et al.⁸**Table S14.** Prices of the main inputs consumed in the processes.

Inputs	Value	Reference
Low pressure steam	\$11.3/t	Cost of opportunity based on the electricity that could be produced with LP steam in condensing turbines
NaOH	\$526/t	Davis et al. ⁸
SrCO ₃	\$810/t	Average US import price in 2016\$ ¹⁴
CO ₂	\$43/t	Adjusted to 2016\$ from Davis et al. ¹⁵
Natural gas	\$3.5/MMBTU	Klein et al. ¹⁶
Electricity	\$0.0682/kWh	Davis et al. ⁸

Table S15. Numerical data corresponding to Figure 9. Values are in dollars per kg monomer.

Cost	NaOH 10 g/L	Sr(OH) ₂ 10 g/L	Sr(OH) ₂ , with CO ₂ recycle 10 g/L	NaOH 100 g/L	Sr(OH) ₂ 100 g/L	Sr(OH) ₂ , with CO ₂ recycle 100 g/L
Steam	1.74	1.21	1.21	0.20	0.28	0.28
Base	30.10	10.47	10.47	4.41	2.62	2.62
CO ₂	1.46	0.31	0.00	0.21	0.08	0.00
Natural gas	0.00	0.21	0.21	0.00	0.05	0.05
Electricity	0.23	0.21	0.21	0.07	0.12	0.12
Capital costs	0.73	0.81	0.81	0.83	1.39	1.39
Total	34.26	13.21	12.91	5.71	4.54	4.46

Table S16. Sensitivity analysis towards lignin oxidation conditions using 100 g/L lignin loading and no CO₂ recycle.

Parameters	Baseline Sr-based process	Milder Sr-based process
Pressure (bar)	60	30
Temperature (°C)	160	175
Residence time (min)	30	10
Monomer yield	5.6%	3.6%
Results		
Processing costs (\$/kg of monomers)	3.96	5.29

Table S17. Numerical data corresponding to Figure 10.

Metric	NaOH 10 g/L	Sr(OH) ₂ 10 g/L	Sr(OH) ₂ , with CO ₂ recycle 10 g/L	NaOH 100 g/L	Sr(OH) ₂ 100 g/L	Sr(OH) ₂ , with CO ₂ recycle 100 g/L
GWP kg CO ₂ /kg	84.8	60.7	46.9	12.2	15.4	11.7
CED MJ/kg	1849.3	1259.0	1180.9	252.6	315.0	294.5
Ecotoxicity DALY/kg	5.28E-05	9.27E-05	8.84E-05	7.65E-06	2.33E-05	2.22E-05

References

1. J. Sluiter and A. Sluiter, *Summative mass closure. Laboratory Analytical Procedure (LAP) Review and Integration*. NREL/TP-510-48087, 2010.
2. B. Cao, L. A. Adutwum, A. O. Oliynyk, E. J. Luber, B. C. Olsen, A. Mar and J. M. Buriak, *ACS Nano*, 2018, **12**, 7434-7444.
3. P. O. Saboe, E. G. Tomashek, H. R. Monroe, S. J. Haugen, R. L. Prestangen, N. S. Cleveland, R. M. Happs, J. Miscall, K. J. Ramirez, R. Katahira, E. C. D. Tan, J. Yan, N. Sun, G. T. Beckham and E. M. Karp, *In Press*, 2022.
4. D. Salvachúa, A. Z. Werner, I. Pardo, M. Michalska, B. A. Black, B. S. Donohoe, S. J. Haugen, R. Katahira, S. Notonier, K. J. Ramirez, A. Amore, S. O. Purvine, E. M. Zink, P. E. Abraham, R. J. Giannone, S. Poudel, P. D. Laible, R. L. Hettich and G. T. Beckham, *Proc. Natl. Acad. Sci. U. S. A.*, 2020, **117**, 9302-9310.
5. C. del Cerro, E. Erickson, T. Dong, A. R. Wong, E. K. Eder, S. O. Purvine, H. D. Mitchell, K. K. Weitz, L. M. Markillie, M. C. Burnet, D. W. Hoyt, R. K. Chu, J.-F. Cheng, K. J. Ramirez, R. Katahira, W. Xiong, M. E. Himmel, V. Subramanian, J. G. Linger and D. Salvachúa, *Proc. Natl. Acad. Sci. U. S. A.*, 2021, **118**, e2017381118.
6. D. G. Brandner, J. S. Kruger, N. E. Thornburg, G. G. Facas, J. K. Kenny, R. J. Dreiling, A. R. C. Morais, T. Renders, N. S. Cleveland, R. M. Happs, R. Katahira, T. B. Vinzant, D. G. Wilcox, Y. Román-Leshkov and G. T. Beckham, *Green Chem.*, 2021, **23**, 5437-5441.
7. S. D. Mansfield, H. Kim, F. Lu and J. Ralph, *Nature Protocols*, 2012, **7**, 1579-1589.
8. R. E. Davis, N. J. Grundl, L. Tao, M. J. Bidy, E. C. Tan, G. T. Beckham, D. Humbird, D. N. Thompson and M. S. Roni, *Process Design and economics for the conversion of lignocellulosic biomass to hydrocarbon fuels and coproducts: 2018 biochemical design case update; biochemical deconstruction and conversion of biomass to fuels and products via integrated biorefinery pathways*. NREL/TP-5100-71949, National Renewable Energy Lab (NREL), 2018.
9. LTS, *Journal*, 2020.
10. *Journal*, 2020.
11. D. D. Hsu, D. Inman, G. A. Heath, E. J. Wolfrum, M. K. Mann and A. Aden, *Environ. Sci. Technol.*, 2010, **44**, 5289-5297.
12. P. Fantke, M. Bijster, C. Guignard, M. Hauschild, M. Huijbregts, O. Jolliet, A. Kounina, V. Magaud, M. Margni, T. E. McKone, L. Posthuma, R. K. Rosenbaum, D. van de Meent and R. van Zelm, *Journal*, 2017.
13. M. Fache, B. Boutevin and S. Caillol, *ACS Sustainable Chem. Eng.*, 2016, **4**, 35-46.
14. S. A. Singerling and J. A. Ober, in *2016 Minerals Yearbook*, United States Geological Survey, 2018.
15. R. Davis, J. Markham, C. Kinchin, N. Grundl, E. C. Tan and D. Humbird, *Process design and economics for the production of algal biomass: algal biomass production in open pond systems and processing through dewatering for downstream conversion*, National Renewable Energy Lab.(NREL), Golden, CO (United States), 2016.
16. B. Klein, I. McNamara, R. Davis, A. Mittal and D. Johnson, *Techno-Economic Assessment for the Production of Hydrocarbon Fuels via Catalytic Upgrading of Furans*. NREL/TP-5100-80652, National Renewable Energy Lab.(NREL), Golden, CO (United States), 2021.